



JOINT INSTITUTE FOR NUCLEAR RESEARCH

Frank Laboratory of Neutron Physics

FINAL REPORT ON THE
SUMMER STUDENT PROGRAM

Research on $n + {}^{12}\text{C}$ reaction at 14.1 MeV

Supervisors:

Dr. Yu.N. Kopatch

Technical assistance:

N.A. Fedorov

Student:

Ilya Dashkov, Russia
Lomonosov Moscow State University

Participation period:

July 1 - August 23

Dubna 2019

Contents

1	Introduction	1
1.1	Processes in reaction $n+^{12}\text{C}$	2
1.2	Hoyle state in ^{12}C	4
2	Nuclear reaction program TALYS	6
2.1	Description	6
2.2	Total reaction cross section for the energy range	9
2.3	Angular distributions	13
3	Tangra setup	17
4	Conclusion	20

Abstract

This work is dedicated to research of nuclear processes occurring in $n+^{12}\text{C}$ reaction. Nuclear reaction program TALYS was used to reproduce experimental results gained from TANGRA experiment and other sources. An experimental setup TANGRA (TAGged Neutron and Gamma RAYs) for studying neutron-induced nuclear reactions is operated by Frank Laboratory of Neutron Physics (FLNP) of the Joint Institute of Nuclear Research (JINR). TANGRA provides experimental data of angular and energy distributions for gamma quanta emitted from a target. Results of TALYS calculation in comparison with experimental data are discussed.

1 Introduction

Neutron-induced reactions are useful to study elemental and isotopic composition of different samples, investigation of the mechanism of these reactions provides possibility to improve our knowledge about structure of atomic nuclei. An experiment called TANGRA at FLNP JINR is dedicated to $(n, x\gamma)$ -type reaction study. The experimental setup used in this project allows one to measure angular and energy distributions of gamma quanta emitted from a target. To interpret results of the experiments carried out on TANGRA setup, the usage of some model calculations is required. Final results of TANGRA work are angular distribution and cross section of inelastically scattered neutrons. That is why good reproduction of these values is a crucial point for verification of the model calculations. The main task of the Summer Practice is to learn the TALYS code and to investigate a possibility of calculations the angular distributions of neutrons and γ -rays, which are measured at TANGRA.

TANGRA collaboration studied a wide variety of samples, but it was decided to focus on calculation for $n+^{12}\text{C}$ reaction. Carbon-12 is rather well studied nucleus with strong, distinguishable 4.44 MeV gamma-line. That is the reason for it to be chosen for this work.

Usually interpretation of mentioned data is not a trivial task. For that programs which realize different theoretical approaches are widely used. One of such programs is TALYS. We decided to use for calculations TALYS 1.9 [1], as it is very versatile and includes many different models. The program uses optical model, DWBA (Distorted Wave Born Approximation) and coupled-channels model for direct reactions, Hauser-Feshbach and width-fluctuation models for compound reactions, several models for nuclear level densities.

1.1 Processes in reaction $n+^{12}\text{C}$

For full interpretation of data coming from TANGRA experiment, it is necessary to evaluate contribution of different reactions and channels to observed picture. In case of fast neutrons with kinetic energy of 14.1 MeV, there could occur different processes with different probability and products.

Neutron inelastic scattering always leads to rise of internal energy of initial nucleus. The excited nucleus can decay by emission of different particles. Probability of each emission is dictated by laws of conservation and quantum rules. By looking at the spectra of participating nuclei one can roughly predict energy spectra and intensities of emitted particles.

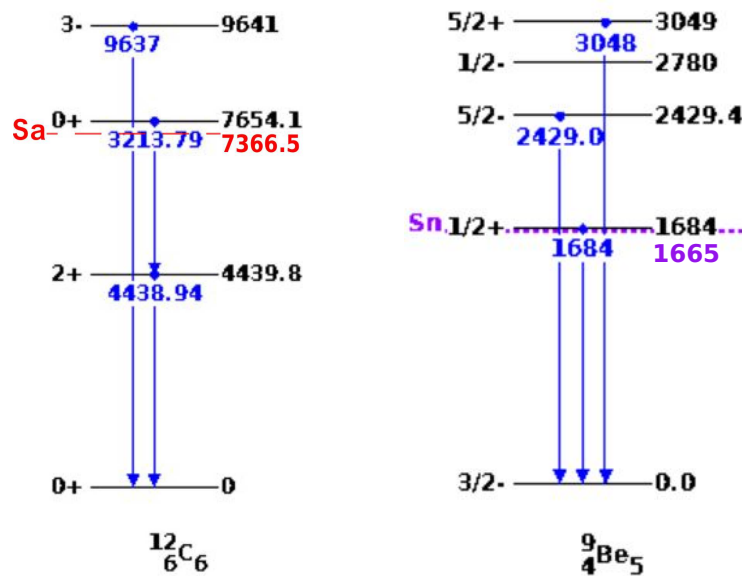


Figure 1: Scheme of ^{12}C and ^9Be levels and gamma transitions. Sa, Sn – alpha-particle and neutron separation energies.

In fig 1 the levels of ^{12}C , ^9Be and gamma transitions between their levels are shown. The first excited state (4.44 MeV) of ^{12}C relaxes by gamma ray transmission. The second (7.65 MeV) and the third (9.64 MeV) emit α -particle with probability of around 100%. Due to low neutron separation energy for ^9Be (1.66 MeV) most of its excited states emit neutron but not gamma-rays. Considering this, one can expect for 4.44 MeV line to be the only one detectable in the neutron irradiation of the ^{12}C .

It is necessary to look at the energy characteristics of the reactions to get a

general idea about their probabilities. All else being equal the greater the reaction energy Q , the more likely it happens. Also the thresholds of the reactions should be considered. Some processes require more kinetic energy of the neutron, than used 14.1 MeV.

Table 1: Some processes in reaction $n+^{12}\text{C}$, their energies, thresholds, and excitation energy of the final nucleus.

Reaction	Excitation energy, MeV	Q , MeV	E_{thr} , MeV
$(n, n)^{12}\text{C}$	0	0	0
$(n, n')^{12}\text{C}^*$	4.44	-4.44	4.81
$(n, n')^{12}\text{C}^*$	7.65	-7.65	8.31
$(n, n')^{12}\text{C}^*$	9.64	-9.64	10.45
$(n, \alpha_0)^9\text{Be}^*$	0	-5.70	6.18
$(n, \alpha_1)^9\text{Be}^*$	1.68	-7.39	8.01
$(n, \alpha_2)^9\text{Be}^*$	2.43	-8.13	8.88
$(n, \alpha_3)^9\text{Be}^*$	2.78	-8.48	9.20
$(n, 3\alpha + n')$	--	-7.28	7.89
$(n, \gamma)^{13}\text{C}$	0	4.95	0
$(n, p)^{12}\text{B}$	--	-12.59	13.84
$(n, d)^{11}\text{B}$	--	-13.73	14.89

The possible neutron induced reactions on carbon with some relevant energy parameters are listed in table 1. Table 1 starts with elastic scattering reaction (n, n) . In this process, the internal energy of the target nucleus does not change, and new particles are not born. Next are the inelastic scatterings (n, n') to different excited states of ^{12}C . The energy level of the final nucleus is shown in the second column. After that there are (n, α) reactions for different excitation of ^9Be . The subscript of the alpha-particle corresponds to the serial number of the excited level of the final nucleus. Zero corresponds to the ground state and then the number increases by one for each subsequent energy level.

Table 1 states, that the dominating processes due to the energy benefit in the reaction should be (n, n) , (n, γ) , they have non-negative Q . Reactions (n, n') ,

$(n, 3\alpha + n')$ are following next. In reality, however, some of the mentioned reaction channels have lower probability to occur.

1.2 Hoyle state in ^{12}C

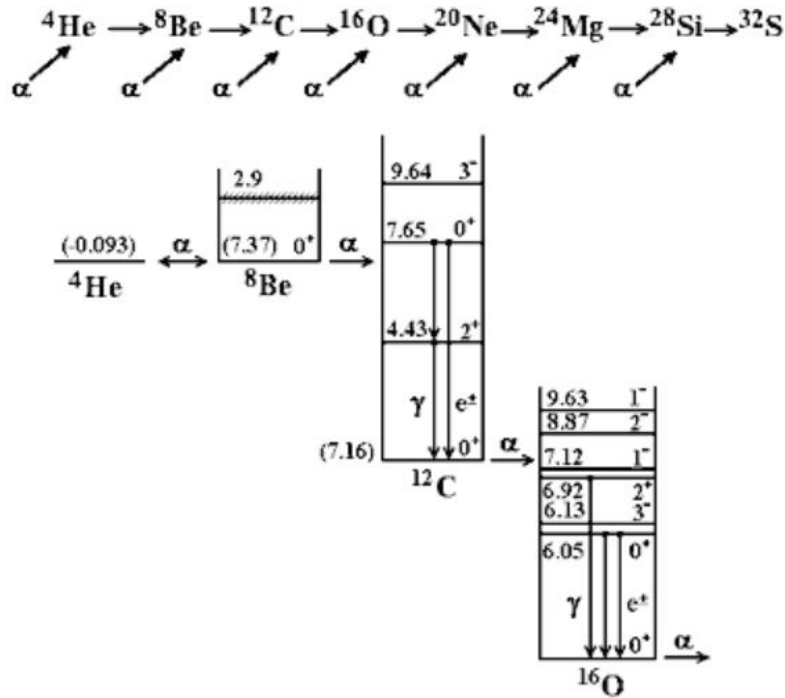


Figure 2: Scheme of α -process in stars. Low levels of ^8Be , ^{12}C , ^{16}O are shown.

An excited ^{12}C level with a spin and parity of 0^+ at 7.65 MeV was predicted by Hoyle to explain the abundance of carbon during nucleosynthesis. Hydrogen in a star burning to produce helium through a series of (p, γ) reactions and β^+ emissions. Helium in turn, should be a link, leading to the birth of heavier elements. But ^8Be , that is born in fusion of two α -particles almost instantly ($< 10^{-15}$ seconds) breaks up to initial particles. Situation becomes different in case of three α -particles fuse together, ^{12}C is stable in the ground state. But the chances of three alpha-particles fuse together without intermediate steps are too low. That is why this option cannot explain the exist amount of the elements heavier then ^4He . Hoyle proposed a process which solves the problem. In the proposed process reaction $\alpha + ^8\text{Be} \rightarrow ^{12}\text{C}^*$ produces ^{12}C in excited state with 7.65 MeV energy. After birth carbon-12 with low probability emits gamma quanta and ends at the ground state.

Then carbon-12 captures one more alpha-particle and produce oxygen-16 in an excited state. That kind of process continues and produces nuclei with number of nucleons equal to a sum of several α -particles (see fig 2).

In cluster model ^{12}C nucleus can be represented as the union of 3 α particles. In the ground state, they, by common belief, make up a triangle. And in the Hoyle state, most likely, a line or bended line (although this interpretation has some problems). The fact is that the charge radius of carbon in the Hoyle state turned out to be very large (the Hoyle state's volume is $\approx 3 - 4$ times larger than the ground state). This can be explained by the quasi-free state of three alpha particles.

Carbon-12 in Hoyle state with high probability breaks up into 3 α -particles. That is why this state can be an important source of alpha-particles in neutron induced reaction on carbon. The total production of α -particles is caused by $(n, 3\alpha + n')$, (n, α) , $(n, n')^{12}\text{C}_{7.65}^*$ and ^8Be breaking up to 2 α -particles. Several sources of α -particles can lead to misjudgment of cross section for corresponding reactions.

2 Nuclear reaction program TALYS

2.1 Description

TALYS [1] is a nuclear reaction program. It's objective is to provide a complete and accurate simulation of nuclear reactions in the 0.001 – 200 MeV energy range, through an optimal combination of reliable nuclear models.

Basic nuclear model, used in TALYS to perform calculations, is a nuclear optical model. The concept of an optical potential with both real and imaginary components was introduced to describe the elastic scattering of neutrons. The central assumption underlying the optical model is that the complicated interaction between an incident particle and a nucleus can be represented by a complex mean-field potential, which divides the reaction flux into a part covering shape elastic scattering and a part describing all competing non-elastic channels. Solving the Schrödinger equation numerically with this complex potential yields a wealth of valuable information. It returns a prediction for the basic observables, namely the elastic angular distribution and polarization, the reaction and total cross section and, for low energies, the potential scattering radius. The quality of the not directly observable quantities that are provided by the optical model has an equally important impact on the evaluation of the various reaction channels.

All optical model calculations are performed by ECIS-06 [2], which is used as a subroutine in TALYS. The default optical model potentials (OMP) used in TALYS are the local and global parameterisations of Koning and Delaroche [3]. Global optical model parameters for ^{12}C nucleus are listed in table 2.

Table 2: Default global optical parameters for neutrons and protons used in TALYS 1.9.

	V_v , MeV	W_v , MeV	r_v , fm	a_v , fm	W_D , MeV	r_D , fm	a_D , fm	V_{SO} , MeV	W_{SO} , MeV	r_{SO} , fm	a_{SO} , fm	r_C , fm	V_C , MeV
n	49.07	1.26	1.13	0.68	7.65	1.31	0.54	5.39	-0.07	0.90	0.59	--	--
p	50.14	1.22	1.13	0.68	7.77	1.31	0.52	5.45	-0.06	0.90	0.59	1.54	2.95

Besides the phenomenological OMP, it is also possible to perform TALYS calculations with the semimicroscopic nucleon-nucleus spherical optical model potential as described in [4]. TALYS uses Eric Bauge's MOM code [5] as a subroutine to perform so called Jeukenne-Lejeune-Mahaux (JLM) OMP calculations. MOM stands

for "Microscopic Optical Model" and in TALYS 1.9, only spherical JLM OMP's are included. The MOM module reads the radial matter densities from the nuclear structure database and performs the folding of the Nuclear Matter (NM) optical model potential described in [4] with the densities to obtain a local OMP. This is then put in the ECIS-06 routine to compute observables by solving the Schrödinger equation for the interaction of the projectile with the aforementioned OMP. The OMP's are calculated by folding the target radial matter density with an OMP in nuclear matter based on the Brückner-Hartree-Fock work of Jeukenne, Lejeune and Mahaux.

The more general coupled-channels method should be invoked to describe simultaneously the elastic scattering channel and the low-lying states which are, due to their collective nature, strongly excited in inelastic scattering. These collective excitations can be described as the result of static or dynamic deformations, which cause the homogeneous neutron-proton fluid to rotate or vibrate. The associated deformation parameters can be predicted from a (semi-)microscopic model or can be derived from an analysis of the experimental angular distributions. In general various different channels, usually the ground state and several inelastic states, are included in a coupling scheme while the associated coupled equations are solved.

The Distorted Wave Born Approximation (DWBA) is only valid for small deformations. Until the advent of the more general coupled-channels formalism, it was the commonly used method to describe inelastic scattering, for both weakly and strongly coupled levels. Nowadays, we see DWBA as a first order vibrational model for small deformation, with only a single iteration to be performed for the coupled channels solution. The interaction between the projectile and the target nucleus is modeled by the derivative of the OMP for elastic scattering times a strength parameter.

In TALYS, DWBA is used if a deformed OMP is not available or if a deformed OMP is used for the first excited states only. First case applies for the spherical OMPs, which are all based on elastic scattering observables only. Hence, if we have not constructed a coupled-channels potential, TALYS will automatically use (tabulated or systematical) deformation parameters for DWBA calculations. In second case DWBA is used with small deformation parameters for the levels that do not belong to that basic coupling scheme, e.g. for the many states at somewhat higher excitation energy.

It is important to distinguish process, which leads to the exit channel of the reaction. It can be direct reaction or compound nucleus. The contributions of two components in elastic and inelastic angular distributions obtained from TALYS are shown in fig 4.

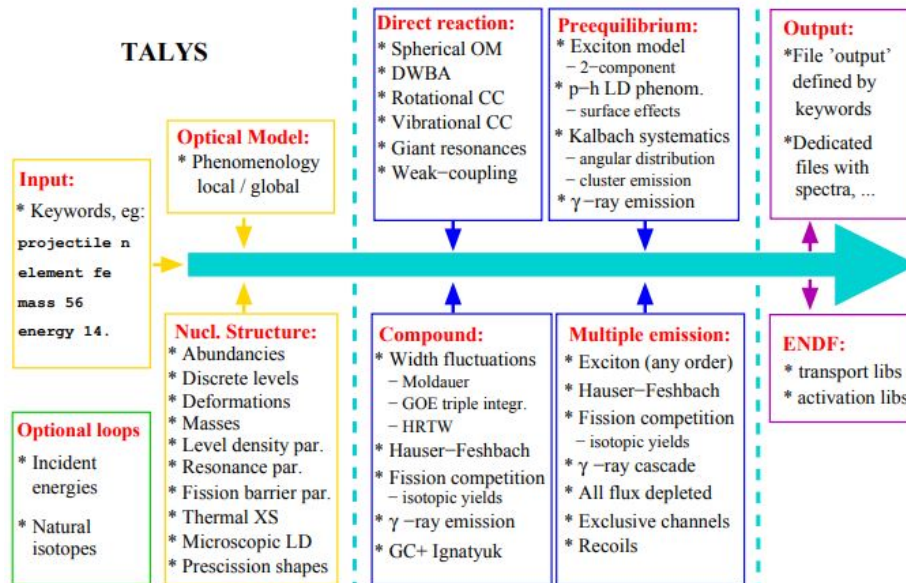


Figure 3: Scheme of TALYS processing its calculation with mentioned models, which are used.

In the case of direct process incident neutron interacts only with a small number of nucleus nucleons. This process is described in the calculation by optical model. A clear anisotropy is observed in the direct component of angular distribution, most neutrons are scattered at small angles below 60° .

Compound component or evaporation spectrum is described by so-called "compound nucleus model". In this case incident neutron excite the whole nucleus. In the first order of approximation this model states, that the collision and particle emission are independent processes. Since the composite core "forgets" the way it is formed, the spectra become symmetric around 90° .

To start TALYS one needs to construct an input file. Input file defines the particles involved in the reaction, the models used, the parameters of these models and the completeness of the output file. Vast number of keywords for the input file makes TALYS parameters pretty flexible. To obtain more precise result, we varied TALYS parameters for different models and turned on some additional keywords. The difference between "best" set of parameters for carbon-12 and default one seems negligible (difference occurs in the third significant figure). Also changing model for width fluctuation corrections in compound nucleus calculations with keyword "widthmode" and model for nuclear level densities with keyword "ldmodel" doesn't show any improvement. The same goes for changing phenomenological optical

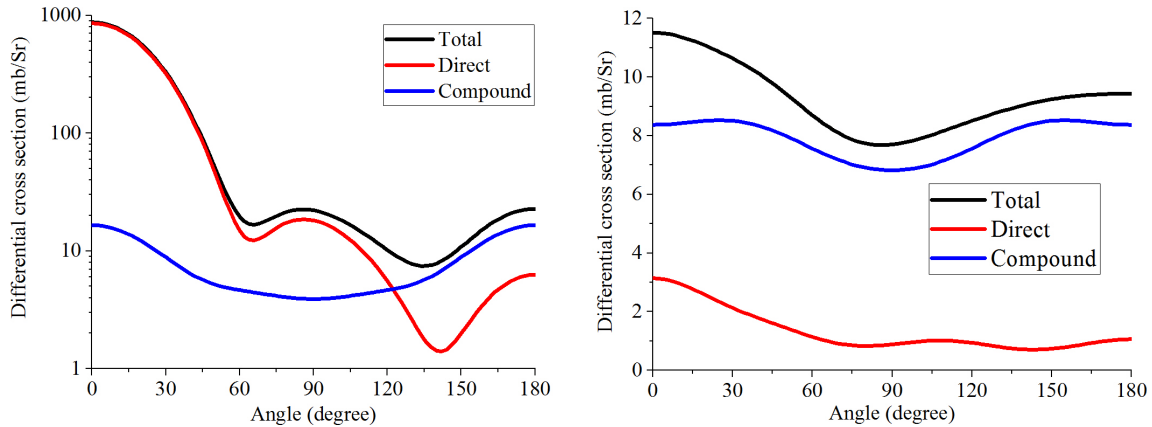


Figure 4: Direct and compound components in elastic (on the left) and inelastic to level 4.44 MeV of ^{12}C (on the right) angular distributions of scattered neutrons at energy 14.1 MeV calculated by TALYS 1.9. Scattering angle is in the laboratory system.

model to semi-microscopic optical model (JLM) [4]. In the least case inelastic cross section rises up, that makes inelastic angular distribution a little closer to the experimental data in general, but makes it worse near minimum (see fig. 11).

2.2 Total reaction cross section for the energy range

TALYS supports wide range of incident energies. Calculation of integral reaction cross sections for different incident energies was performed. In this section TALYS 1.9 results for cross sections are compared with different experimental sources. The data and references were received from the EXFOR library. The results are listed in fig. 5-9.

Fig. 5 shows us, that in range of 5 – 20 MeV TALYS result is close to ENDF estimation and experimental data. TALYS gives larger (around 20% more at 14 MeV energy) than ENDF total cross section for the discussed reaction in this range. But in the same time TALYS remains within the margin of error for experimental data.

Almost the same picture is occurred for elastic scattering cross section, that is seen in fig. 6. For the range of 0.5 – 20 MeV TALYS is generally close to the experimental values and ENDF estimations.

For the cross section of all inelastic channels (non-elastic cross section) see fig. 7. The lack of experimental data (there is only one point on the graph) makes it impossible to compare the results obtained from TALYS with something other than the ENDF score. In comparison with it, TALYS overestimates the cross section for

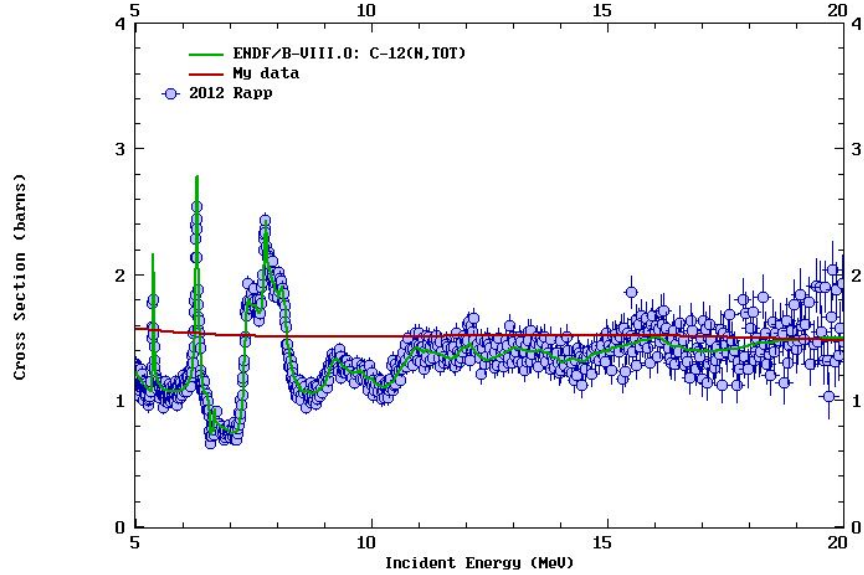


Figure 5: Total neutron scattering on carbon-12 cross section for energies from 5 up to 20 MeV. Points are experimental data. Green line is the estimation adopted in the ENDF/B-VIII.0 database. The bordeaux line is the result of calculating the section using TALYS.

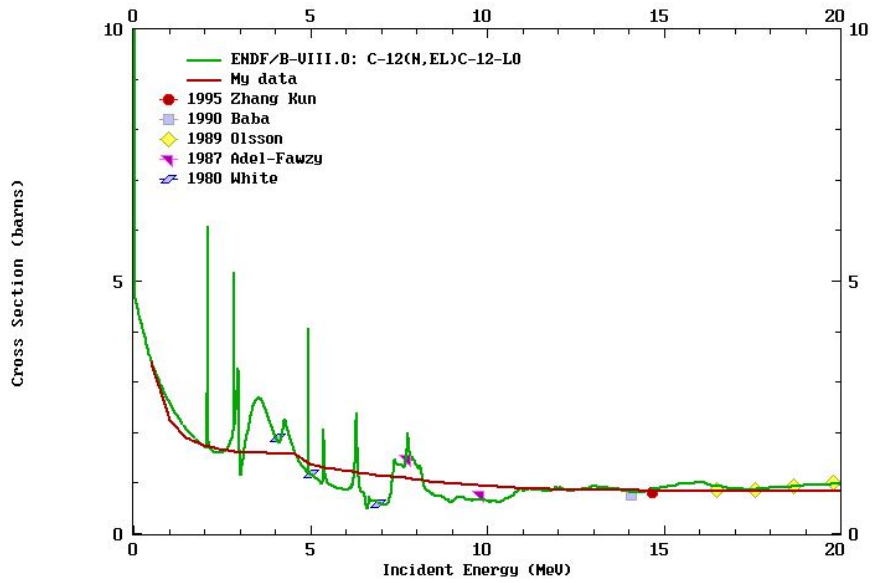


Figure 6: Elastic neutron scattering on carbon-12 cross section for energies up to 20 MeV. Points are experimental data. Green line is the estimation adopted in the ENDF/B-VIII database. The bordeaux line is the result of calculating the section using TALYS.

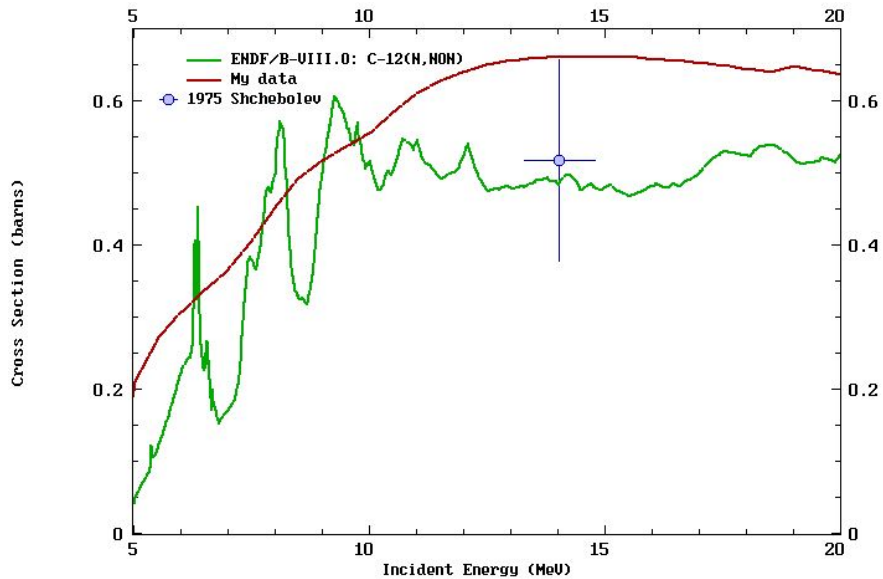


Figure 7: Cross section of all inelastic channels for neutrons collided with carbon-12 at energies of 5–20 MeV. Red line is the estimation adopted in the ENDF/B-VIII database. The black line is the result of calculating using TALYS 1.9.

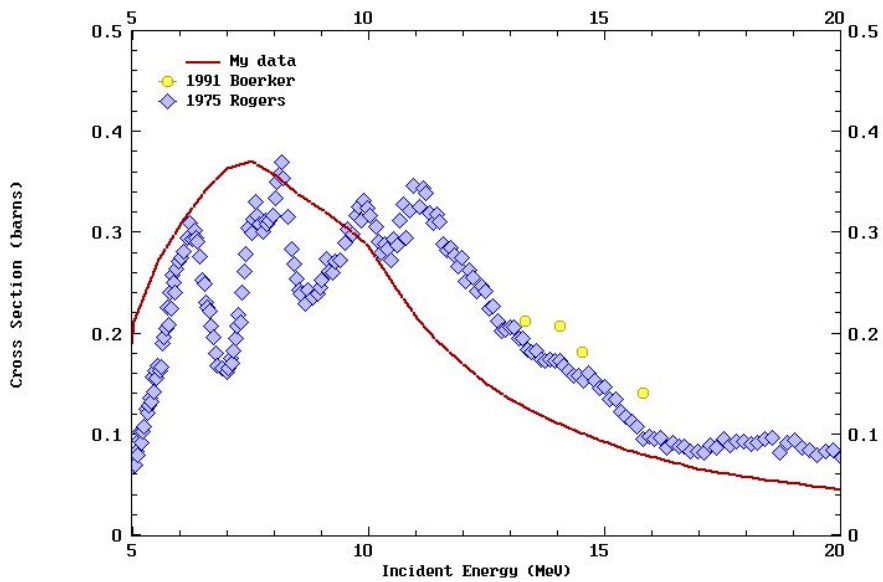


Figure 8: Inelastic neutron scattering cross section for energies 0–20 MeV to the first excited level (4.44 MeV) of ^{12}C . The bordeaux line is the result of calculating the section using TALYS.

the interval from 11 to 20 MeV by an average of 0.15 barn.

Exfor does not produce experiments where the inelastic scattering integral cross section has been measured. But there are partial, for example, to the first excited level (4.44 MeV) of ^{12}C . The data for the integral inelastic scattering cross section are presented as neutron scattering cross sections corresponding to the first excitation levels ^{12}C .

Fig. 8 shows, that for the first excited level of 4.44 MeV TALYS reproduces general trend in cross section behavior. But it doesn't reproduce absolute value of integral cross section. For the point at 14 MeV TALYS underestimate cross section in approximately 1.5 times.

In addition to scattering cross sections, it is important to closely reproduce cross section of (n, α) reaction.

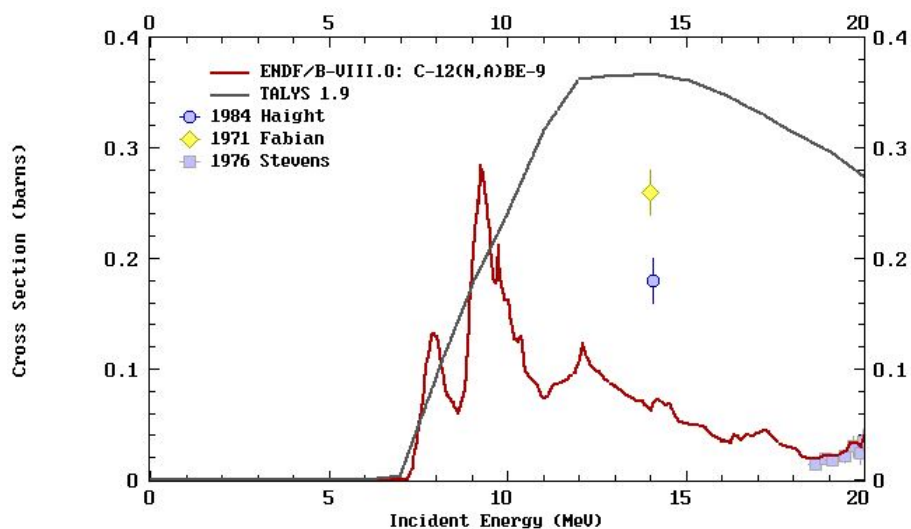


Figure 9: Cross section of (n, α) reaction for energies 0 – 20 MeV. Points are experimental data. Bordeaux line is the sectional estimate adopted in the ENDF/B-VIII database. Black line is the result of calculating cross sections by using TALYS.

The EXFOR library does not have enough information about experimental measurements of (n, α) reaction cross sections. It can be seen in the fig. 9 that TALYS overestimates the integral cross section by about 4 times in comparison with the ENDF estimate at neutron energies close to the investigated 14.1 MeV.

For all the graphs in this section, it can be seen that TALYS is generally close to the experimental values and the accepted estimate of the total integral cross section for all the reactions considered. However, it completely ignores the fine structure

of the spectrum without reproducing the cross section peaks.

In table 3 integral cross sections from experiments conducted on energies close to 14.1 MeV and result of TALYS calculation. Based on the table, TALYS is good at reproducing total, elastic alpha-particle production integral cross sections. Taking the closest experimental values, calculated ones differ by less than 10%. While the cross sections of scattering to the 4.44 MeV excited carbon state and of (n, α_0) reaction differ from experimental by 0.6 and 1.3 times respectively. It is important to note, that experiments sometimes give different results for the same reactions and incident energies. That is why evaluation of the accuracy of the program depends on the selected reference experimental data.

2.3 Angular distributions

In this subsection angular distributions of reaction products gained from TALYS 1.9 are compared with experimental results.

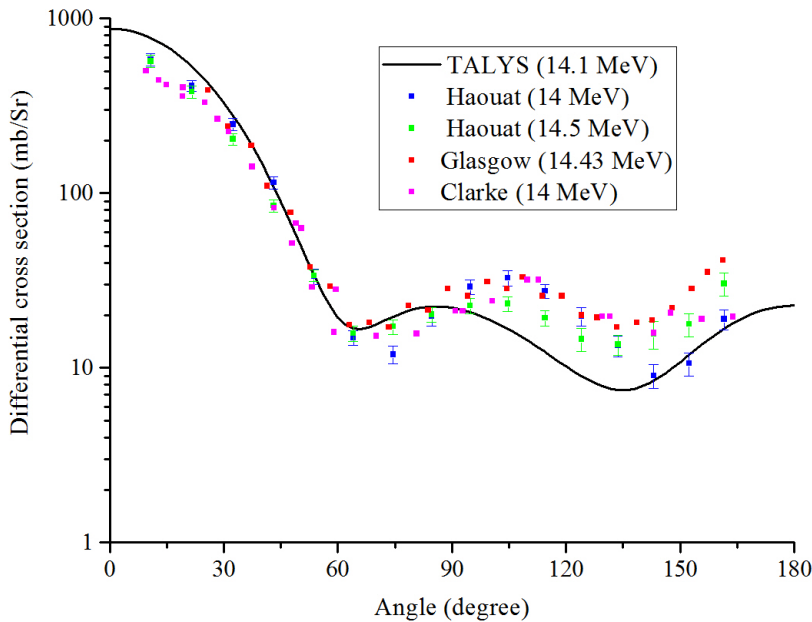


Figure 10: Calculated angular distribution of elastic neutron scattering for energies close to 14.1 MeV. Scattering angle is in the laboratory system.

Fig 10 shows, that TALYS on a logarithmic scale almost coincides with experimental data for angles up to 90° . At the same time TALYS noticeably underestimates values for angles greater than 90° . Pretty reliable result of TALYS is no

Table 3: Integral cross sections of reactions, occurring in neutron scattering on ^{12}C .

Reaction	Incident energy, MeV	Cross section, mb	Reference
(n, tot)	14.1	1524	TALYS 1.9
	14	1480 ± 100	[6]
(n, n)	14	793 ± 35	[7]
	14.5	717 ± 35	[7]
	14.1	864	TALYS 1.9
(n, n')	14.1	299	TALYS 1.9
$(n, n')^{12}\text{C}_{4.44}^*$	14	184 ± 8	[7]
	14.5	146 ± 8	[7]
	14.7	214 ± 8	[8]
	14.1	110	TALYS 1.9
$(n, n')^{12}\text{C}_{7.65}^*$	14.7	9.3 ± 1.6	[8]
	14.1	20	TALYS 1.9
$(n, n')^{12}\text{C}_{9.64}^*$	14.1	67	TALYS 1.9
$(n, * + \alpha)$	14.1	402 ± 46	[9]
	14.8	900 ± 70	[10]
	14.4	654 ± 92	[11]
	14.9	744 ± 60	[11]
	14.1	366	TALYS 1.9
(n, α_0)	14.1	62 ± 15	[12]
	14.2	69 ± 6	[13]
	14.5	69 ± 13	[14]
	14.1	21 ± 5	[15]
	13.9	79 ± 20	[16]
	14.1	76 ± 11	[17]
	14.1	72 ± 9	[9]
	14.1	81	ENDF/B-V
	14.1	88	TALYS 1.9
(n, α_1)	14.1	44	TALYS 1.9
(n, α_2)	14.1	77	TALYS 1.9
$(n, n'3\alpha)$	14.1	–	TALYS 1.9
	14	301 ± 89	[18]
	14.1	190 ± 20	[19]
	14.2	202 ± 30	[20]
	14.1	110 ± 15	[9]

surprise, because it uses optical model. Description of the elastic scattering process in optical model coincides well with experimental data [21].

It follows from Fig 11 that TALYS systematically overestimates the value of the inelastic neutron scattering cross section by about 200 mb in comparison with the ENDF estimation.

Fig 12 shows, that TALYS gives a little larger (less than 4 mb/Sr larger) cross sections for angular distributions of alpha particle in (n, α_0) . Also calculation doesn't reproduce differential cross-section increase around 90° , which is observed in [9] and [13].

The contribution of the (n, γ) reaction to the birth of gamma rays is not significant. There are no experimental data about that total cross section. TALYS gives negligible 0.02 mb for (n, γ) reaction.

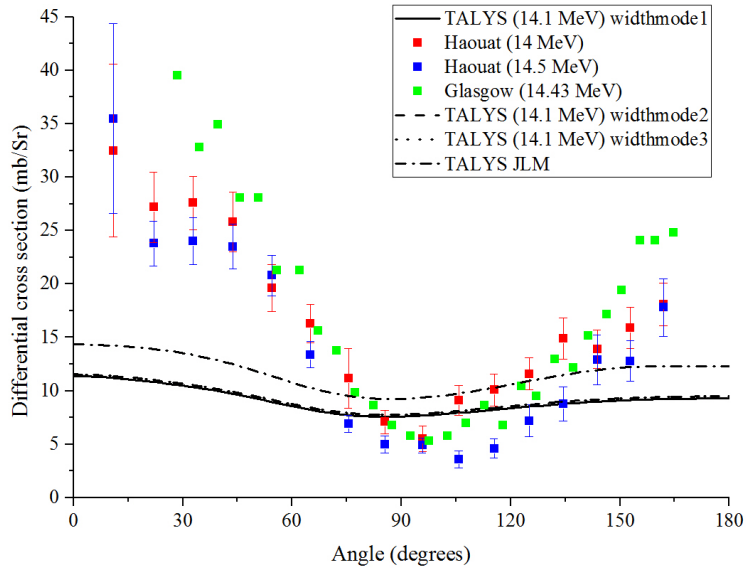


Figure 11: Differential angular cross section for inelastic neutron scattering to first excited state (4.44 MeV) of carbon. Scattering angle is in the laboratory system.

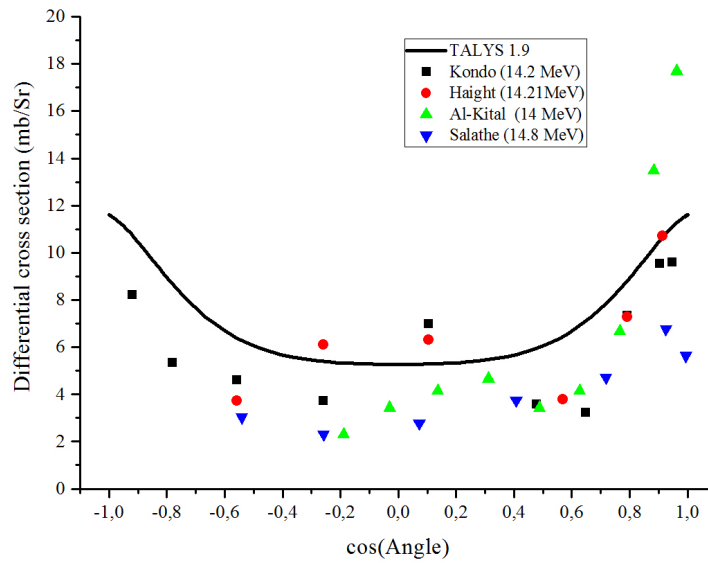


Figure 12: Differential angular cross section for (n, α_0) reaction. The black line is TALYS 1.9 calculation result, dots are experimental results. Scattering angle is in the laboratory system.

3 Tangra setup

The construction of the experimental setup ROMASHA (see fig 13) allows one to study the angular distribution of gamma quanta, a very important characteristic of inelastic scattering process, which provides information about the nature of the neutron-nucleus interaction and allows to determine its mechanism (a reaction through compound nucleus or via direct reaction). This aspect is discussed in detail in [22]. For higher energy resolution the HPGe detector is used. The setup scheme with the HPGe detector is shown in fig. 14.

The setup consists of: a portable neutron generator ING-27 [23], a compact dismountable collimator, an array of gamma spectrometers (currently a configuration of Ge gamma detector is used) and a 32-channel data acquisition system based on a personal computer equipped with expansion cards with ADC.

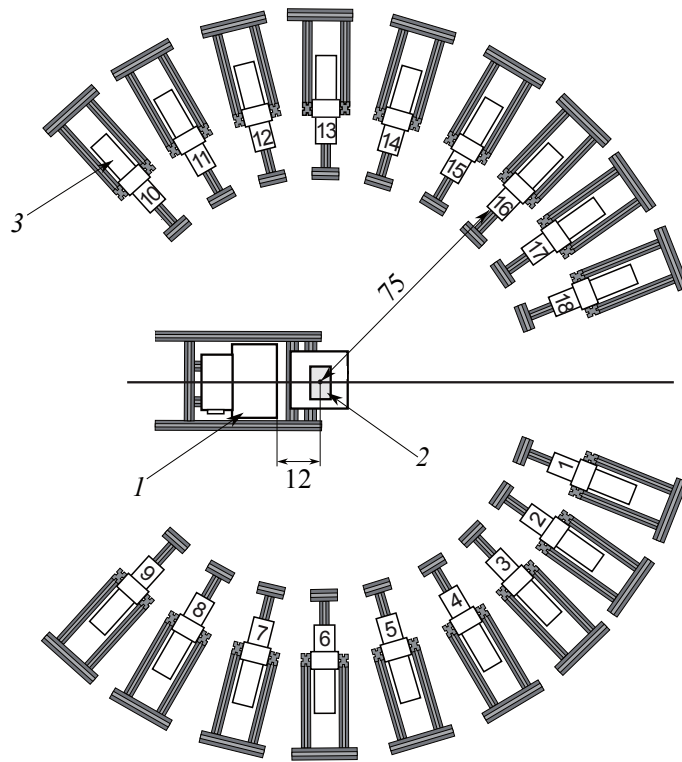


Figure 13: TANGRA BGO Romasha scheme. The numbers denote: 1 - neutron generator ING-27, 2 - sample, 3 - BGO detector. The distances are in centimeters.

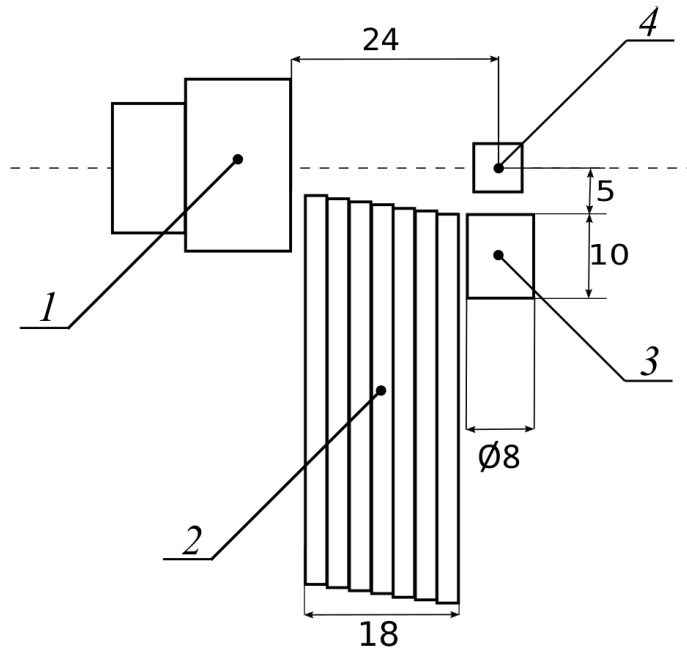


Figure 14: TANGRA HPGe scheme. The numbers denote: 1 - neutron generator ING-27, 2 - collapsible lead shield, 3 - HPGe gamma detector, 4 - sample. The distances are in centimeters.

One of the most important features of TANGRA experiment is usage of tagged neutrons. The Tagged Neutrons Method (TNM) is widely known experimental method. The main idea of this approach is quite simple: the neutrons are produced in a d-t fusion reaction:



The products of this reaction, the alpha particle and the neutron, fly in opposite directions; the alpha-particle can be simply detected and its direction can be determined, therefore the direction of the neutron can be established, too. If the neutron interacts with the target nucleus it can excite it in an inelastic scattering process in which the nucleus emits gamma-rays. The ordinary time interval between the neutron scattering and the emission of gamma quanta is very short, therefore the space coordinates of interaction point can be estimated.

ING-27 is a computer-controlled neutron generator designed and manufactured at the All-Russian Scientific Research Institute of Automation named after N.L. Duhov. The intensity of the neutron flux produced by this generator reaches $5 \times 10^7 \text{c}^{-1}$. A simplified diagram of the neutron generator is shown in fig. 15.

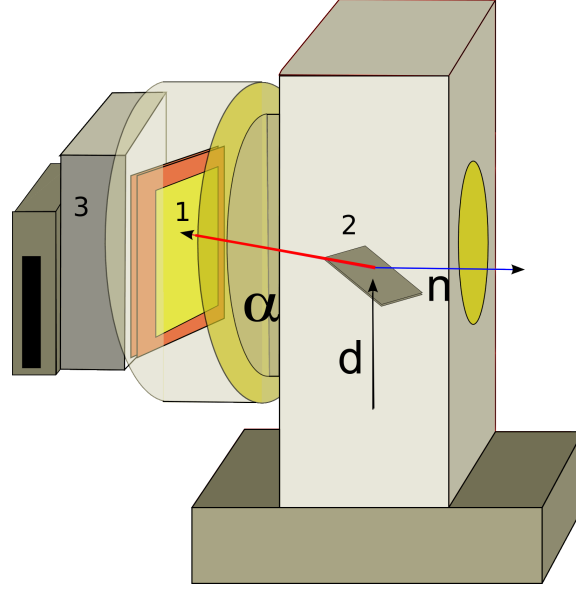


Figure 15: The scheme of the neutron generator. The numbers indicate: 1 - pixel α -detector, 2 - target enriched with tritium, 3 - block preamplifier.

The main element of the generator is a sealed neutron tube filled with deuterium, with a built-in pixel alpha detector. The generation of neutrons inside this tube occurs as a result of the reaction (1). The energy of the neutron can be obtained by the formula, the conclusion of which is widely known:

$$T_n = \frac{m_d m_n T_d}{(m_n + m_\alpha)^2} (\cos \theta_n + \sqrt{\cos^2 \theta_n + \frac{(m_n + m_\alpha)[(m_\alpha - m_n)T_d + m_\alpha Q]}{m_d m_n T_d}})^2 \quad (2)$$

where T_d is the kinetic energy of the incident deuteron, and the θ_n is the emission angle of the neutron in the laboratory reference frame relative to the axis of the deuteron beam. Calculations give us the difference between the maximum and minimum neutron energies ≈ 0.01 MeV. Thus, it turns out that the spectrum of tagged neutrons with good accuracy can be considered monochromatic.

Since the reaction products are only two particles, according to the law of conservation of momentum, they scatter in opposite directions (in the center of mass system). Therefore, by registering the direction of flight of one of the particles, we

can find out the direction of flight of the second particle. This property of the reaction is the basis of the tagged neutron method.

TANGRA gives gamma-quantum cross section for 4.44 MeV line of 130 ± 15 mb. While TALYS for the same parameter gives 167 mb.

4 Conclusion

TALYS is a comprehensive program for nuclear reaction calculation and has rich number of variable parameters. Even so, TALYS seems to be unusable to our concrete tasks. TALYS cannot correctly reproduce angular inelastic distribution of neutrons for 4.44 MeV excited carbon state. Also TALYS does not calculate at all the angular distribution of the γ -ray emitted from the inelastically excited nucleus. To alter the situation a deep modernization of the software is needed.

Acknowledgments

I would like to thank the University Center of the Joint Institute for Nuclear Research and the Management of the Frank Laboratory for Neutron Physics for the financial support of my summer practice and the excellent working atmosphere during all my stay in Dubna.

Also, I have to express out appreciation to my scientific supervisors, Dr. Yu.N. Kopatch and Dr. I.N. Ruskov for their patience, motivation, and immense knowledge. I am also immensely grateful to N.A. Fedorov for his invaluable assistance in performing of this work.

References

- [1] A. J. Koning *et al.* TALYS-1.9 A nuclear reaction program User Manual (2017)
- [2] J. Raynal, Notes on ECIS94, CEA Saclay Report No. CEA-N-2772, (1994)
- [3] A. J. Koning and J.P. Delaroche, "Local and global nucleon optical models from 1 keV to 200 MeV", Nucl. Phys. A713, p. 231–310 (2003)
- [4] E. Bauge *et al.*, Phys. Rev. C 63, p. 024607 (2001)
- [5] R. Capote *et al.*, "RIPL - Reference Input Parameter Library for calculation of nuclear reactions and nuclear data evaluation", Nucl. Data Sheets 110, 3107 (2009)
- [6] Rapp, M. J., *et al.* "Beryllium and Graphite Neutron Total Cross-Section Measurements from 0.4 to 20 MeV", Nuclear Science and Engineering, 172(3), p. 268–277. (2012)
- [7] G. Haout *et al.* Nuclear Science and Engineering 65, p. 331-346 (1978)
- [8] K. Gul *et al.* Physical Review C 24, 6, (1981)
- [9] R. C. Haight *et al.* Nuclear Science and Engineering 87, 1, p. 41–47 (1984)
- [10] G. R. Farrar *et al.* Physics Letters B, Vol. 76, Issue 5, p. 575–579 (1978)
- [11] J. B. Holt *et al.* Proc. Mtg. Technology of Controlled Nuclear Fusion, Richland, Washington, September 21-23, CONF-760935, p. 1565, U.S. Energy Research and Development Administration (1976)
- [12] R. A. Al-Kital, R. A. Peck, Jr., " $^{12}\text{C}(n, \alpha)\text{Be}^9$ reaction induced by 14-MeV neutrons", Phys. Rev., 130, 1500 (1963)
- [13] K. Kondo *et al.*, Journal of Nuclear Science and Technology, Vol. 45, No. 2, p. 103–115 (2008)
- [14] M. L. Chatterjee *et al.* Nuclear Physics 51, p. 583–587, (1964)
- [15] D. Kopsch and S. Cierjacks, Nucl. Instrum. Methods 54, p. 277 (1967)
- [16] M. Brendle, *et al.* "The $^{12}\text{C}(n, \alpha_0)^9\text{Be}$ reaction at 13.9 and 15.6 MeV", Z. Naturforsch., 23a, p. 1229 (1968)

- [17] H. Kitazawa, N. Yamamuro, " (n, α) Reaction on ^{12}C induced by 14.1 MeV neutrons", J. Phys. Soc. Japan, 26, p. 600 (1969)
- [18] B. Antolkovic *et al.*, Nucl. Phys., A394, p. 87 (1983)
- [19] G. A. Grin *et al.*, Helv. Phys. Acta, 42, p. 990 (1969)
- [20] F. Cocu *et al.*, "Sections Efficaces Differentiates et Totale de la Reaction $^{12}\text{C}(n, n'3\alpha)$ a $E_n = 14.2$ MeV," CEA-R-4746, Centre d'Etudes de Bruyeres-le-Chatel (1976)
- [21] H. F. Lutz *et al.* "Optical model analysis of scattering of 14 MeV neutrons by light nuclei", Lawrence Radiation Laboratory, University of California, Livermore, California (1963)
- [22] B. A. Benetskii and I. M. Frank, "Angular correlation between gamma rays and 14-MeV neutrons", JETP, 17, 1963, p. 309-313
- [23] Neutron generators for analysis of substances and materials. ING-27 gas-filled neutron tube based neutron generator of VNIIA, http://www.vniia.ru/eng/production/incl/prospekt_element_eng.pdf